

## The Role of Silica Nanofluid as a Plugging Agent for Enhanced Oil Recovery – Experimental Approach

Al Muhannad Al Omairi<sup>1</sup>, Girma Tadesse Chala<sup>1,\*</sup>

<sup>1</sup> Department of Mechanical Engineering (Well Engineering), International College of Engineering and Management, P.O. Box 2511, C.P.O Seeb, P.C. 111, Muscat, Oman

### ARTICLE INFO

#### Article history:

Received 20 September 2023

Received in revised form 11 November 2023

Accepted 23 December 2023

Available online 31 January 2024

#### Keywords:

Nanoparticles; silica nanoparticles;  
enhance oil recovery; plugging

### ABSTRACT

Many enhanced oil recovery techniques have been adopted in oil production to recover as much oil as possible. However, enhanced oil recovery techniques are complex and costly. Therefore, nanofluids have been modified in the laboratory to be consistent with reservoir fluids and rocks while also being environmentally benign. This study aims to investigate the role of silica nanofluid in plugging the high permeable zones after oil is recovered from the reservoir to divert pressure to the low permeable zone for enhanced oil production from the low permeable zones. A digital gas permeameter (DGP-300-B) was used to determine the permeability of the core by injecting nitrogen gas. In addition, a DHP-100-M Digital Helium Porosimeter was used to determine bulk volume, grain volume, and grain density porosity. The experiment was conducted with different percentages of silicon dioxide nanoparticles to observe the effect of plugging in each stage. Results show that a 52% reduction in core permeability was observed when using 0.5wt.% of silica nanoparticles, a 72% reduction in core permeability when using 1wt.% of silica nanoparticles and a 94% reduction in core permeability when using 2wt.% of silica nanoparticles.

## 1. Introduction

Tertiary recovery, also known as Enhanced Oil Recovery (EOR), is generally divided into four major types:

- i. thermal which includes hot water, steam and combustion
- ii. gas injection consisting of hydrocarbon, CO<sub>2</sub> and nitrogen/flue
- iii. chemical involving alkali, surfactants and polymers
- iv. other techniques such as microbial, acoustic and electromagnetic [1,2].

The quickest way to increase oil output and maintain the total oil production plateau is to drill new wells one after another; however, this approach is expensive and several environmental risks

\* Corresponding author.

E-mail address: [girma@icem.edu.om](mailto:girma@icem.edu.om)

are involved, particularly with hydraulic fracturing [3,4]. As a result, Enhanced Oil Recovery (EOR) possibilities are being examined and a few pilots using CO<sub>2</sub> and hydrocarbon gas injection have recently been done in the United States, primarily using the single well huff-n-puff technique [5]. All EOR methods intend to lower the saturation level of oil lower than the residual level of oil saturation [6].

Although nanotechnology is not an EOR approach in and of itself, the unique properties at the nanoscale enable current methods to function better [7]. The distinctive qualities of nanoparticles, such as superior surface-to-volume ratio, reduced interfacial tension and wettability control, can be attributed to this modification in petroleum engineering [8,9]. Nanoparticles must be adsorbed onto the rock surface to affect its wettability [10]. The inclusion of nanoparticles has been hypothesized to alter two potential underlying mechanisms for the improvement in contact line motion. The pressure gradient generated by the "wedge" fluid in the area of the nanoparticle adsorbed onto the solid surface, or three-phase contact line, reduces friction [7].

Nanotechnology has been touted as a propitious agent for EOR approaches from both an environmental and economic standpoint. The capacity of NPs to penetrate the pore throat, the capability to decrease interfacial tension, and the optimal rise in the viscosity of aqueous solution led to a reasonable adjustment of reservoir parameters for improved oil mobility. Different oil displacement mechanisms, such as rock surface wettability alteration, formation of structural disjoining pressure, interfacial, phase analysis and surface tension decline events, have also been explored and introduced [11].

Experiments show that increased disjoining forces depend on the size and number of nanoparticles; thinner nanoparticles with more significant amounts offer a stronger repulsive force [12]. Mcelfresh *et al.*, Wasan *et al.*, Chengara *et al.*, and Wasan and Nikolov [13-16] have all conducted investigations and highlighted that nanoparticles in the three-phase zone between water, oil and rock tend to stick together. They push their way through the discontinuous phase onto solid rock surface. Nanoparticles are tiny particles made up of atoms and molecules, forming a wedge-shaped structure separating the formation fluid from the pore wall. It improves the nano fluid's spreading tendency [17].

An experimental investigation by Bila *et al.*, [18] showed that the wettability of the cores was shifted from powerfully water/wet to neutral/wet during the ageing process. The major oil was produced earlier than a breakthrough point, but there was further oil production as the injection progressed, indicating that the nanofluid systems have significant EOR potential. When nanoparticles are added to the oil-water combination, interfacial tension (IFT) lowers because of enhanced adhesion forces among the injected fluids and remaining oil, resulting in oil recovery. Surfactants such as sodium dodecyl sulphate were also utilized in nanofluid to change the IFT. It appears that combining SiO<sub>2</sub> nanoparticles with brine oil is a smart idea because they can gain less IFT and produce more oil. IFT influences capillary number, adhesion tension and capillary pressure, according to Fan and Buckley. As IFT declined, the capillary number improved, freeing some remaining oil. Small-size nanoparticles have a larger surface area, increasing the nanoparticles' contact with the oil phase, allowing for greater recovery. Silica nanoparticles are the most often utilized nanoparticles in EOR (SiNPs) [19].

Silicon dioxide, the major sandstone component, makes up 99.8% of silica nanoparticles. When compared to other nanomaterials, silica nanoparticles are a more environmental option. Furthermore, silica nanoparticles are inexpensive, and their chemical activity may be regulated by altering their surface [20-22]. The IFT has been shown to be affected by silica hydrophilic nanoparticles. Nanoparticles migrate to the interface, reducing the amount of oil in contact with the brine. Surfactants work similarly, but on a different principle. The lattice-Boltzmann approach was

used to describe the mechanisms of neutral particle adsorption, which were then compared to those of surfactants. Because of their well-known amphiphilic features, surfactants adsorb at the liquid/liquid interface, whereas neutral wetting nanoparticles adsorb because maintaining a particle–fluid contact needs less energy. This behaviour can be explained in terms of the system's free energy. Moreover, the appeal between NPs and gas-liquid interface is thought to aid in limiting NPs loss to the rock formation, and silica NPs are likely to outlast traditional surfactants in harsh reservoir conditions [7].

Because of its low-priced fabrication and simplicity of modifying the surface, silica nanofluids have recently gained popularity in the oilfield [23]. When dispersed in a solution, the dissolved NPs are susceptible to agglomeration, forming aggregates [24]. Grain agglomeration is a method to reduce surface free energy by enlarging NP aggregates and decreasing nanoparticles' surface area.

Cao *et al.*, [25] effectively manufactured three nano silica particles modified with varying content of a hydrophobic group. Unlike nano-silica particles, modified nanoparticles ensured good emulsification, stability and interface qualities. It also sustained the emulsion for an extended time and at elevated temperatures. Furthermore, at a concentration of 1000 mg/L, it shifted the oil-wet core to balanced wetting, lowering interfacial tension from 14.9 to 10.4 mN/m. Furthermore, in the micro-displacement experiment, the modified nanoparticle dispersed across a larger region with the displacement recovery approaching 41.4 %, indicating that it has a significant ability to EOR.

The recovery potential and stability of SNF was studied in a recent study at various nanoparticle concentrations (0.1, 0.07, 0.05, 0.02wt%) and salinities of 20 thousand, 30 thousand, and 40 thousand ppm [26]. The test was split into two parts: the optimum concentration of NP had been determined at 20 thousand ppm, and the salinity effect on the recovery mechanisms was investigated. The first set of trials attained the best recovery and displacement efficiency at a concentration of 0.05wt percent. Because of the changes in the recovery process, displacement and recovery efficiency reduce as the concentration rises. The nanofluid instability and a shift from chemical to mechanical blocking processes are responsible for the low recovery. More tests were conducted at higher salinities, such as 20 thousand, 30 thousand, and 40 thousand ppm. As salinity rises to 30 thousand ppm, recovery decreases, but at 40 thousand ppm, recovery increases. According to Mittal 2021, SiO<sub>2</sub> nanoparticles have been proven to boost oil recovery in high-salinity conditions. Most experiments conducted earlier in EOR using silica nanoparticles present the amount of oil recovered from sweeping the oil. However, limited studies have been available investigating the role of silica nanofluid as a plugging agent for enhanced oil recovery. Therefore, this study aims to examine the influence of silica nanofluid as a plugging agent in the recovery processes.

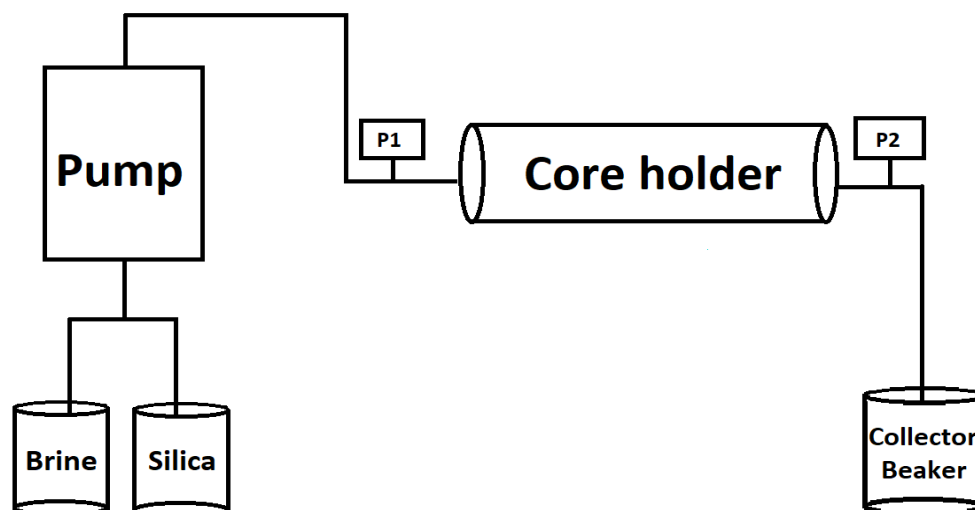
## 2. Experimental Techniques

### 2.1 Materials and Methods

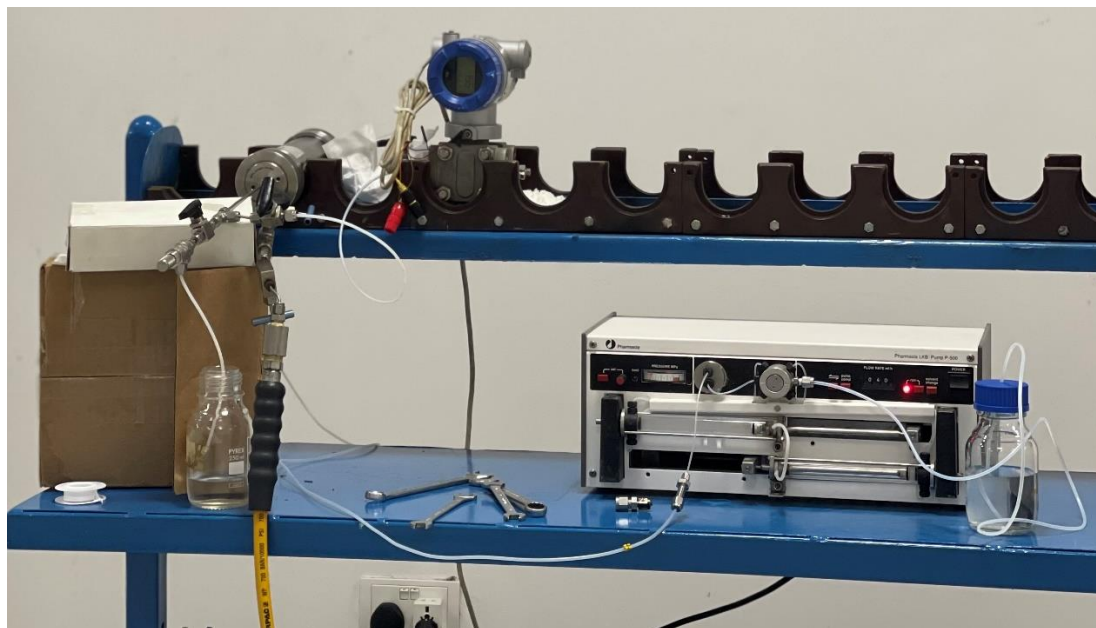
The core used in this study is a sandstone Berea core with a weight of 130.13g, a diameter of 3.77cm and a length of 6.36cm. Digital gas perimeter (DGP-300-B) was used to determine the permeability of the core by pumping 400psi of nitrogen gas into the core. Two pressure sensors in the core holder determined the gas pressure entering and exiting the core, after which the permeability was calculated. The matrix cup contains the core sample using a DHP-100-M Digital Helium Porosimeter. From the reference cell, helium is isothermally expanded into the matrix cup. The reference cell's initial helium pressure was then measured. The volume of the reference cell is known and recorded to measure the equilibrium pressure. Both pressures are measured and displayed visually using a digital transducer. The grain volume was calculated using Boyles' law as the matrix cup cell's original volume is known. Three brine samples are collected and examined at

different temperatures to determine the density and viscosity. EIGA Micromega was used to filter and get ultrapure water to make brine. A magnetic stirrer was used to mix 41.08g/L of NaCl with 3 litres of water to produce brine. After mixing the brine fluid, Glass Microfiber filters were used for turbidity removal and bacterial culture filtration.

A U-tube viscometer was used to determine viscosity by holding it vertically inside a water bath. The first step was to scoop liquid into the capillary tube using the pipette or the wider limb. The fluid is free to flow through the tube. The liquid is poured into the tube until it completely fills bulb 1. The liquid is sucked from the other end of the tube after the bulb-1 has been filled. The liquid begins to move through the U-tube from bulb-1 to bulb-2. When the liquid reaches bulb 2, it can flow easily inside the capillary tube from the upper to the lower marking. A stopwatch was used to time the flow of the liquid from the upper mark to the lower mark. This time was then used to calculate the viscosity of the liquid. The density of the brine was determined by measuring its mass and volume. To improve precision and accuracy, measurements were taken on three brine samples. The mass was measured in grams (g) using an electronic balance, and the volume was measured in millilitres using a graduated cylinder (mL). The core was saturated with brine by using a vessel chamber which is attached to a vacuum pump. The vacuum pump was turned on until it sucks all the air from the core. The vessel was then attached to a bottle of brine to suck the brine from the bottle due to pressure difference, suturing the core with brine. Brine was pumped into the core using a Pharmacia pump to ensure that the core was 100% saturated with brine, and permeability  $K_w$  was measured. The core sample was placed inside a core holder, two pressure sensors were attached to record pressure entering and exiting the core. All pumping operation was done at room temperature 24 (°C). Silica nanofluid was prepared in three different concentrations (0.5, 1, 2wt.%). Sonicate was used to mix silica NPs with brine to make it a homogeneous fluid. The three concentrations of silica fluid are examined in different temperatures to determine the density and viscosity behaviour in different temperatures. Silica fluid was pumped gradually from 0.5wt.% to 2wt.% into the core using a Pharmacia pump, and pressures were recorded. High Precision Pump P-500 was used to pump brine and silica nanofluid into the core with a constant flow pressure ranging from 0 to 600 psi. Figure 1 shows the experimental setup.



(a)



(b)  
**Fig. 1.** Experimental setup: (a) schematic diagram, (b) photographic view

### 3. Results and Discussion

#### 3.1 Permeability and Porosity of the Core Sample

Table 1 shows the core analysis and readings. The permeability of the core sample, calculated by Darcy equations, is 409.098md. This was considered very high in the sandstone permeability classification.

**Table 1**

Core analysis and readings

Weight (g)	Length (cm)	Diameter (cm)	Gas flow reading (Stml/min)	Diff, pressure reading (mbar)	Gas flow (Stml/min)	Diff. pressure	Kg (mD)	KL (mD)
130.13	6.36	3.77	298.9	116.3	298.6	117.1	409.098	381.507

The porosity of the core sample is also depicted in Table 2, where the porosity volume was calculated using Boyles' law.

**Table 2**

Porosity of core sample

Bulk volume (L*A)	Grain volume	Grain density (gm/cc)	Porosity at ambient (%)	Pore volume
70.95	49.92	2.61	29.636	21.03

#### 3.2 Rheological Properties of Brine

##### 3.2.1 Density and viscosity of brine in different temperatures

Brine was used as a base fluid for the experiment to simulate the reservoir conditions. Three brine samples were tested at different temperatures to determine the density and viscosity in each temperature. Figure 2 shows the variation in density and viscosity of brine in different temperatures at 15°C to 26°C. At 15°C the viscosity of brine is 1.2566cP and the density is 1.014450351 g/cm<sup>3</sup>, as

the temperature increases the viscosity decreases and density increases till it reaches a viscosity of 0.9974cP and a density of 1.014913926 g/cm<sup>3</sup> at a temperature of 26°C.

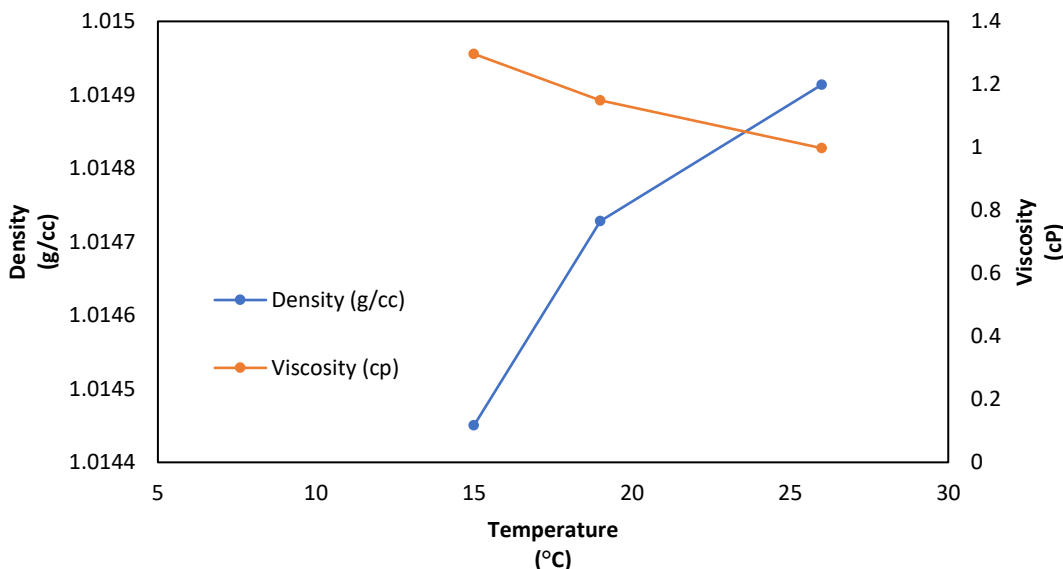


Fig. 2. Brine viscosity and density

### 3.2.2 Pumping brine into the core

Brine was pumped into the core, and the core sample's permeability was measured by the brine, so Kw was determined as a reference before pumping silica nanofluid. The permeability of the core Kw is 98.226mD (Table 3), the reference and most accurate permeability reading for the test. Brine was pumped at a temperature of 24°C, at different flow rates from 64.248 to 93.9 ml/h to get the average permeability.

Table 3

Permeability of brine (Kw)

T (°C)	L (cm)	D (cm)	DP (%)	Q (ml/h)	DP (mbar)	DPcorr (mbar)	L/A (1/cm)	Kw (mD)	Kw_corr (mD)		Kw (mD)
24.00	6.36	3.77	0.50	64.248	99.21	108.70	0.571	107.4	98.045		98.226
24.00	6.36	3.77	0.58	74.132	115.10	124.59	0.571	106.8	98.699	DP/Q	1.689
24.00	6.36	3.77	0.67	84.016	133.00	142.49	0.571	104.8	97.812	DP offset	-9.49
24.00	6.36	3.77	0.75	93.9	148.89	158.38	0.571	104.6	98.350	R2	0.9997

### 3.3 Rheological Properties of Silica Nanofluid

#### 3.3.1 Density and viscosity of 0.5wt% of silica nanofluid

Three samples of 0.5wt.% silica nanofluid are tested in different temperatures to determine the density in each temperature. Figure 3 shows the variation in density and viscosity of 0.5wt.% silica nanofluid in different temperatures at 16°C, 20°C and 24°C. At 16°C the viscosity is 1.2703cP and the density is 1.005114403 g/cm<sup>3</sup>, as the temperature increases the viscosity decreases and density increases till it reaches a viscosity of 1.0939cP and a density of 1.005881689g/cm<sup>3</sup> at a temperature of 24°C.

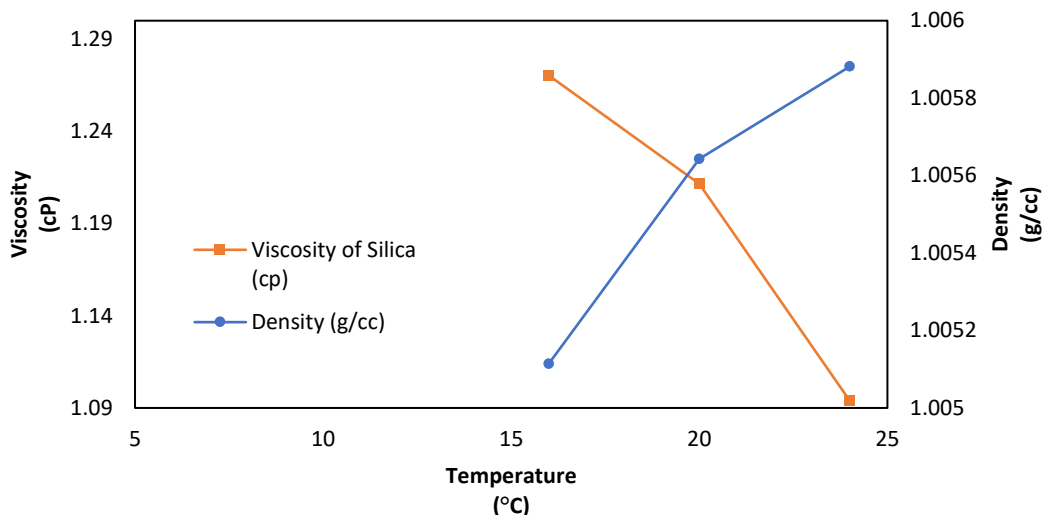


**Fig. 3.** 0.5wt.% Silica nano fluid viscosity and density

Figure 4 shows the viscosity of 0.5wt% silica and brine; there is an increase in the viscosity by 9.7% when 0.5wt.% of silica is added to brine at 24°C.

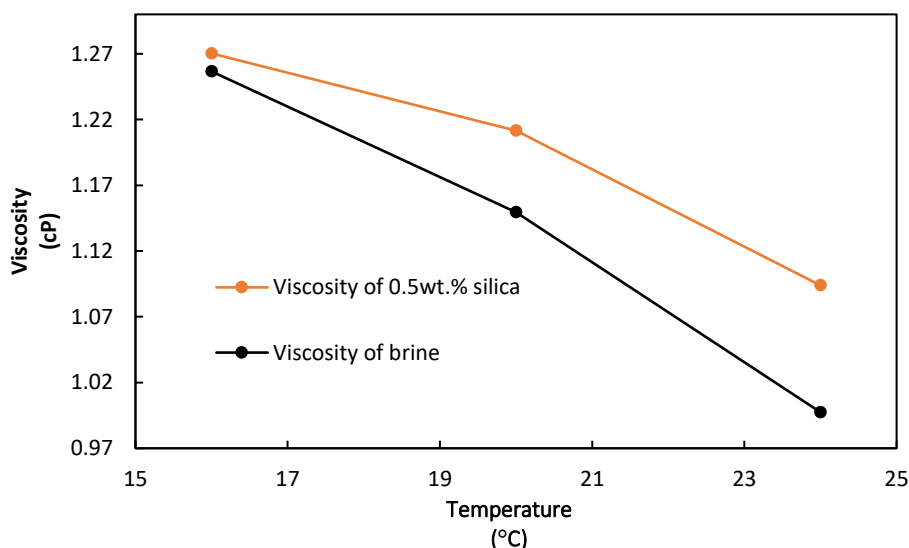


**Fig. 4.** Viscosity of 0.5wt% silica vs brine

### 3.3.2 Density and viscosity of 1wt% of silica nanofluid

Three samples of 1wt.% silica nanofluid are tested in different temperatures to determine the density in each temperature. Figure 5 shows the variation in density and viscosity of 1wt.% silica nanofluid in different temperatures at 15°C, 20°C and 24°C. At 15°C the viscosity is 1.2975cP and the density is 1.000246127g/cm<sup>3</sup>. As the temperature increases, the viscosity decreases and density increases till it reaches a viscosity of 1.1325cP and a density of 1.001181897g/cm<sup>3</sup> at a temperature of 24°C.

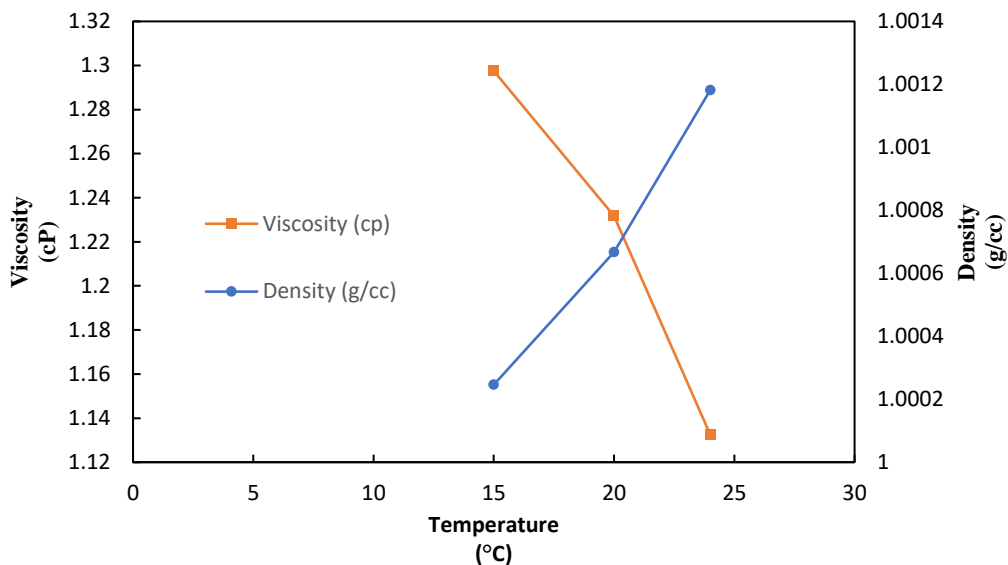


**Fig. 5.** Viscosity and density of silica nanofluid with 1 wt%

Figure 6 shows the viscosity of 1wt% Silica vs Brine Viscosity, there is an increase in the viscosity by 13.5% when 1wt.% of silica is added in brine at 24°C.

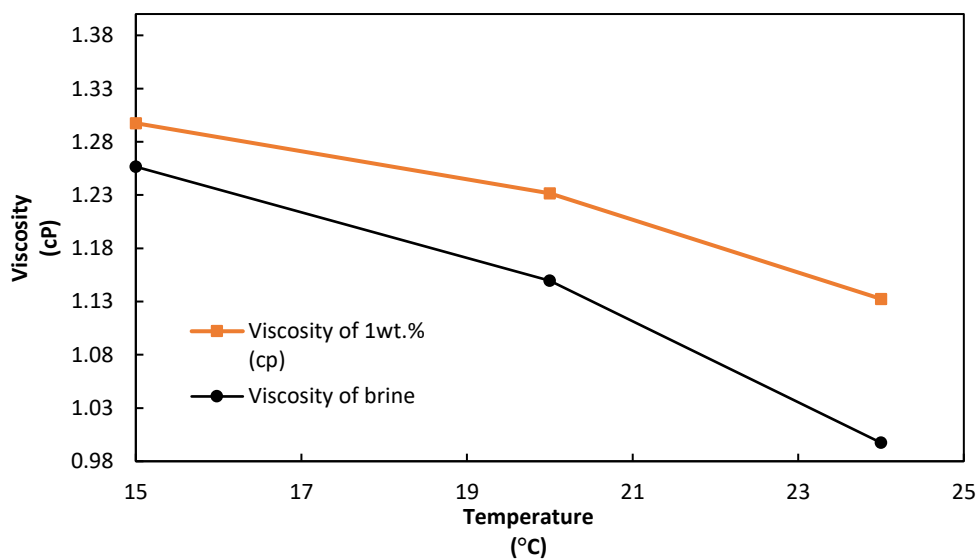


**Fig. 6.** Viscosity of 1 wt% silica vs brine

### 3.3.3 Density and viscosity of 2wt% of silica nanofluid

Three samples of 2wt.% silica nanofluid are tested at different temperatures to determine the density. Figure 7 shows the variation in density and viscosity of 2wt.% silica nanofluid in different temperatures at 15°C, 20°C and 24°C. At 15°C the viscosity is 1.3133cP and the density is 1.002743162g/cm<sup>3</sup>. As the temperature increase the viscosity decreases and density increase till it reaches a viscosity of 1.1589cP and a density of 1.003617836g/cm<sup>3</sup> at a temperature of 24°C.



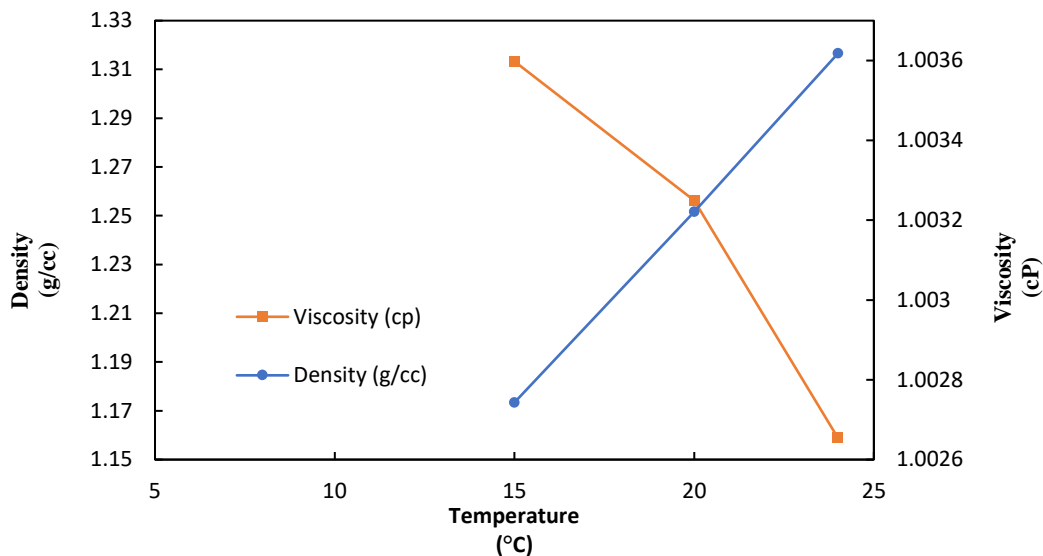


**Fig. 7.** Viscosity and density of 2wt.% silica nanofluid

Figure 8 shows the viscosity of 2wt% silica and brine. There is an increase in the viscosity by 16.2% when 2wt.% of silica is added in brine at 24°C.

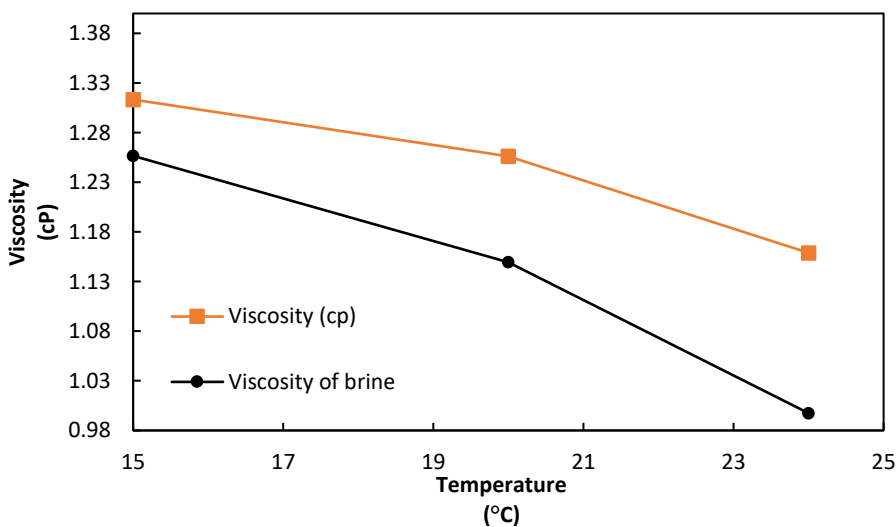


**Fig. 8.** Viscosity of 2wt% silica vs brine

### 3.4 Effect of Different Concentrations of Silica Nanofluid on Viscosity

The effect of different silica nanofluid concentrations on the viscosity in different temperatures is investigated. Figure 9 shows viscosity profiles for different concentrations of silica nanofluid. At the concentration of 0.5wt.% the silica nanofluid viscosity at 24°C is 1.0939cP. As the temperature dropped to 20°C the viscosity increased to 1.2115cP and when the temperature decreased to 16°C the viscosity was the highest at 1.2703cP. As the concentration of silica nanoparticles increased to 1wt.% the viscosity increased to 1.1325cP compared with 0.5wt.% at 24°C as temperature drops to 20°C the viscosity increased to 1.2317cP. The highest viscosity of 1wt.% was noted at 15°C, which is 1.2317cP. At a concentration of 2wt.%, the viscosity of silica nanofluid was the highest at 24°C compared to 0.5wt.% and 1wt.%, which is 1.1589cP. When the temperature decreased to 20°C, the

viscosity increased to 1.2562cP; when the temperature decreased to 15°C, the viscosity was the highest, 1.3133cP. As noticed, the viscosity of silica nanofluid increases as the concentration of silica nanoparticles increases and when the temperature drops the viscosity increases.

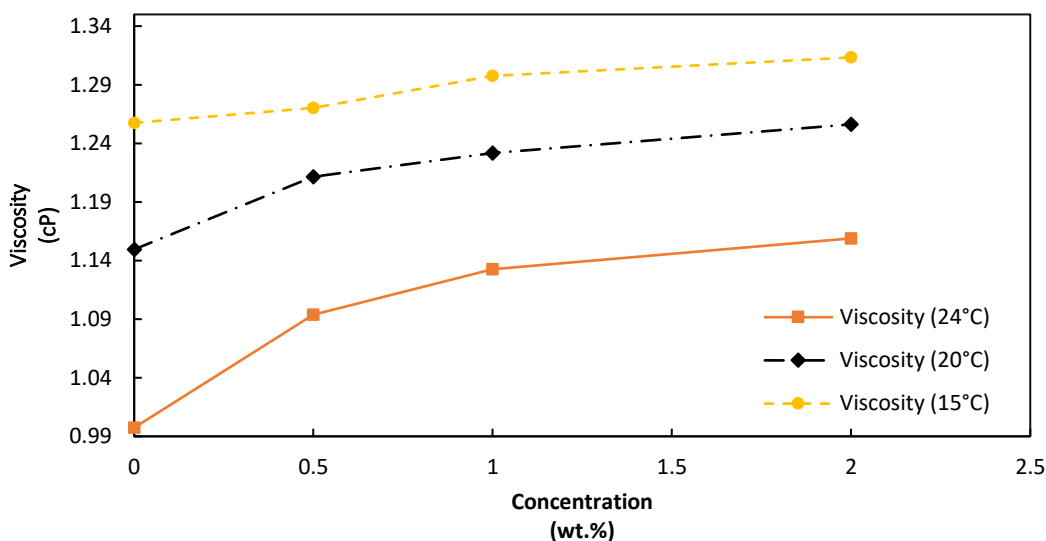


Fig. 9. Effect of different concentrations of silica nanofluid on viscosity

### 3.5 Effect of Different Concentrations of Silica Nanofluid on Plugging

Table 4 shows permeability before and after injecting different concentrations of silica nanofluid.

**Table 4**  
 Effect of concentration of silica nanofluid on plugging

Concentration (wt.%)	Permeability before injecting Silica nano fluid (mD)	Permeability after injecting Silica nano fluid(mD)	Percentage of plugging
0.5wt.%	98	47	52%
1wt.%	98	27	72%
2wt.%	98	6	94%

Figure 10 shows the effects of varying concentrations of silica nanofluid on the plugging. It was observed that the permeability decreases due to plugging as the concentration of silica nanofluid increases. First injection was at a concentration of 0.5wt.%. Silica nanofluid was injected until the differential pressure was stable. The permeability of the core decreased from 98mD to 47mD with a reduction of 52%. Second, 1wt.% of silica nanofluid was injected into the core until the differential pressure was stable; readings showed that the permeability of the core decreased by 72% from 98mD to 27mD. The last injection was carried out in a concentration of 2wt.% of silica nanofluid until it was stable. A significant drop in permeability from 98mD to 6mD was observed, significantly increasing the plugging percentage. The maximum core plugging caused by silica nanofluid injection was 94% at concentrations of 2wt.%. The minimum core plugging was 52% at the concentration of 0.5wt.%. This indicates the improvement in the EOR using silica nanofluid. A study by Youssif *et al.*, also revealed an increase in oil recovery by using a concentration of 0.1wt.% to 0.5wt.% of silica nanofluid to sweep and produce more oil. This was also observed in the study by Li *et al.*,

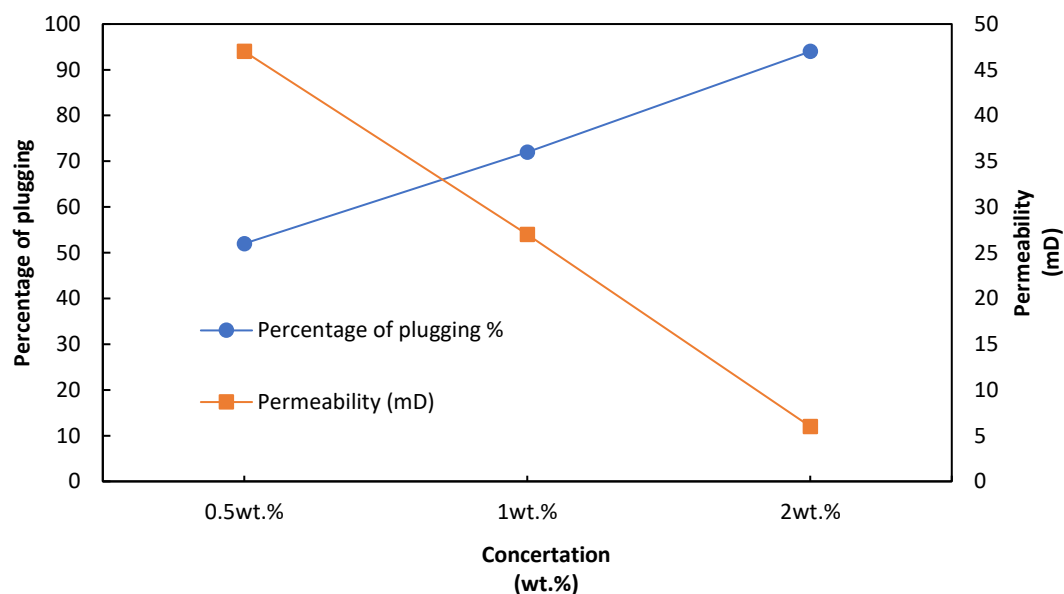


Fig. 10. Effects of concentration of Silica nanofluid on plugging

#### 4. Conclusions

Most experiments conducted in EOR using silica nanoparticles present the amount of oil recovered from sweeping the oil. This study, however, focuses mainly on plugging percentages in different concentrations of silica nanofluid. When different techniques are used to EOR the pressure tends to go through the high permeability zone and diverts away from the low permeability zones. This causes an issue because the oil in low permeability zones is not recovered. When the high permeability zone is plugged, water flooding or any oil recovery method is diverted to the low permeability zone, thus increasing the hydrocarbon displacement through improved sweep efficiency in the low permeability zone. A digital gas permeameter (DGP-300-B) was used to determine the permeability of the core by injecting nitrogen gas. DHP-100-M Digital Helium Porosimeter was used to determine bulk volume, grain volume, and grain density porosity. The experiment was conducted with different percentages of silicon dioxide nanoparticles to investigate the effect of plugging in each stage. It was observed that 52% reduction in core permeability was observed when using 0.5wt.% of silica nanoparticles, 72% reduction in core permeability when using 1wt.% of silica nanoparticles and 94% reduction in core permeability when using 2wt.% of silica nanoparticles. As for plugging the high permeable zone to divert IOR or EOR fluid to low permeable zones or to plug water from entering the production well silica nanofluid can be used in a higher concentration of 1wt.% to 2wt.%.

#### Acknowledgement

The authors would like to thank the Stratum Reservoir company for granting permission to use all necessary equipment and materials to complete the experiment in their lab. The authors would like to thank The Research Council (TRC) Oman for funding this project through the MoHERI/BFP/ICEM/01/21 grant reference code.

#### References

- [1] Abdullahi, Mohammed Bashir, Shiferaw Regassa Jufar, Iskandar Dzulkarnain, Tareq Mohammed Al-shami, and Minh Duc Le. "Seismic Wave Excitation of Mature Oil Reservoirs for Green EOR Technology." *Journal of Advanced*

- Research in Fluid Mechanics and Thermal Sciences* 103, no. 2 (2023): 180-196. <https://doi.org/10.37934/arfmts.103.2.180196>
- [2] Firozjaili, Ali Mohsenatabar, and Hamid Reza Saghafi. "Review on chemical enhanced oil recovery using polymer flooding: Fundamentals, experimental and numerical simulation." *Petroleum* 6, no. 2 (2020): 115-122. <https://doi.org/10.1016/j.petlm.2019.09.003>
- [3] Amer SA, Al Jabri, and T. Chala Girma. "A Review of Challenges in Hydraulic Fracturing Operation." *INTI JOURNAL* 2020, no. 18 (2020).
- [4] Al Jabri, Amer SA, and Girma T. Chala. "Geological Challenges in Hydraulic Fracturing Operation: A Case Study in Undisclosed Petroleum Field in Oman." *Platform: A Journal of Engineering* 4, no. 4 (2020): 18-25.
- [5] Syed, Fahad Iqbal, Temoor Muther, Vuong Pham Van, Amirmasoud Kalantari Dahaghi, and Shahin Negahban. "Numerical trend analysis for factors affecting EOR performance and CO2 storage in tight oil reservoirs." *Fuel* 316 (2022): 123370. <https://doi.org/10.1016/j.fuel.2022.123370>
- [6] Rahman, Musfika, and Iskandar Dzulkarnain. "Response Surface Method for Modelling the Effect of CO2 in Brine/Waxy Oil Interfacial Tension during LSW-WAG Enhanced Oil Recovery." *Journal of Advanced Research in Applied Sciences and Engineering Technology* 22, no. 1 (2021): 54-68. <https://doi.org/10.37934/araset.22.1.5468>
- [7] Druetta, Pablo, Patrizio Raffa, and Francesco Picchioni. "Plenty of room at the bottom: nanotechnology as solution to an old issue in enhanced oil recovery." *Applied Sciences* 8, no. 12 (2018): 2596. <https://doi.org/10.3390/app8122596>
- [8] Rezk, Marwan Y., and Nageh K. Allam. "Impact of nanotechnology on enhanced oil recovery: A mini-review." *Industrial & engineering chemistry research* 58, no. 36 (2019): 16287-16295. <https://doi.org/10.1021/acs.iecr.9b03693>
- [9] Alkalbani, Almotasim K., Girma T. Chala, and Alhaitham M. Alkalbani. "Experimental investigation of the rheological properties of water base mud with silica nanoparticles for deep well application." *Ain Shams Engineering Journal* 14, no. 10 (2023): 102147. <https://doi.org/10.1016/j.asej.2023.102147>
- [10] Alsedrani, Maryam Q., and Girma T. Chala. "Investigation of the Effects of Silica Nanofluid for Enhanced Oil Recovery Applications: CFD Simulation Study." *Arabian Journal for Science and Engineering* 48, no. 7 (2023): 9139-9158. <https://doi.org/10.1007/s13369-022-07113-9>
- [11] Sikiru, Surajudeen, Amir Rostami, Hassan Soleimani, Noorhana Yahya, Yusuf Afeez, Oluwaseyi Aliu, Jemilat Yetunde Yusuf, and Temidayo Lekan Oladosu. "Graphene: outlook in the enhance oil recovery (EOR)." *Journal of Molecular Liquids* 321 (2021): 114519. <https://doi.org/10.1016/j.molliq.2020.114519>
- [12] Mittal, Ajay. "Recent advances in using a silica nanofluid for enhanced oil recovery." *Materials Today: Proceedings* 52 (2022): 1260-1266. <https://doi.org/10.1016/j.matpr.2021.11.050>
- [13] McElfresh, Paul, David Holcomb, and Daniel Ector. "Application of nanofluid technology to improve recovery in oil and gas wells." In *SPE international oilfield nanotechnology conference and exhibition*. OnePetro, 2012. <https://doi.org/10.2118/154827-MS>
- [14] Wasan, Darsh, Alex Nikolov, and Kirti Kondiparty. "The wetting and spreading of nanofluids on solids: Role of the structural disjoining pressure." *Current Opinion in Colloid & Interface Science* 16, no. 4 (2011): 344-349. <https://doi.org/10.1016/j.cocis.2011.02.001>
- [15] Chengara, Anoop, Alex D. Nikolov, Darsh T. Wasan, Andriy Trokhymchuk, and Douglas Henderson. "Spreading of nanofluids driven by the structural disjoining pressure gradient." *Journal of colloid and interface science* 280, no. 1 (2004): 192-201. <https://doi.org/10.1016/j.jcis.2004.07.005>
- [16] Wasan, Darsh T., and Alex D. Nikolov. "Spreading of nanofluids on solids." *Nature* 423, no. 6936 (2003): 156-159. <https://doi.org/10.1038/nature01591>
- [17] Sajjadian, Majid, V. Sajjadianand, and Ali Akbar Daya. "Experimental investigation of using nano fluid to improve productivity index on enhancing oil recovery." *International Journal of Mining Science* 2, no. 2 (2016): 13-19. <https://doi.org/10.20431/2454-9460.0202003>
- [18] Bila, Alberto, Jan Åge Stensen, and Ole Torsæter. "Experimental investigation of polymer-coated silica nanoparticles for enhanced oil recovery." *Nanomaterials* 9, no. 6 (2019): 822. <https://doi.org/10.3390/nano9060822>
- [19] Youssif, Magda I., Rehab M. El-Maghraby, Sayed M. Saleh, and Ahmed Elgibaly. "Silica nanofluid flooding for enhanced oil recovery in sandstone rocks." *Egyptian Journal of Petroleum* 27, no. 1 (2018): 105-110. <https://doi.org/10.1016/j.ejpe.2017.01.006>
- [20] Li, Shidong, Luky Hendraningrat, and Ole Torsaeter. "Improved oil recovery by hydrophilic silica nanoparticles suspension: 2 phase flow experimental studies." In *IPTC 2013: International Petroleum Technology Conference*, pp. cp-350. European Association of Geoscientists & Engineers, 2013. <https://doi.org/10.2523/16707-MS>
- [21] Fakoya, Muili Feyisitan, and Subhash Nandlal Shah. "Emergence of nanotechnology in the oil and gas industry: Emphasis on the application of silica nanoparticles." *Petroleum* 3, no. 4 (2017): 391-405. <https://doi.org/10.1016/j.petlm.2017.03.001>

- [22] Nadim, Muhammad Amirul, Irmie Azlin Zakaria, Baljit Singh Bhathal Singh, Wan Ahmad Najmi Wan Mohamed, and Rosnadiyah Bahsan. "Al<sub>2</sub>O<sub>3</sub> and SiO<sub>2</sub> Nanofluids Performance in Thermoelectric Generator." *Journal of Advanced Research in Fluid Mechanics and Thermal Sciences* 107, no. 1 (2023): 45-57. <https://doi.org/10.37934/arfmts.107.1.4557>
- [23] Sharma, Tushar, and Jitendra S. Sangwai. "Effects of electrolytes on the stability and dynamic rheological properties of an oil-in-water pickering emulsion stabilized by a nanoparticle–surfactant–polymer system." *Industrial & Engineering Chemistry Research* 54, no. 21 (2015): 5842-5852. <https://doi.org/10.1021/acs.iecr.5b00734>
- [24] Raghav Chaturvedi, Krishna, Rakesh Kumar, Japan Trivedi, James J. Sheng, and Tushar Sharma. "Stable silica nanofluids of an oilfield polymer for enhanced CO<sub>2</sub> absorption for oilfield applications." *Energy & Fuels* 32, no. 12 (2018): 12730-12741. <https://doi.org/10.1021/acs.energyfuels.8b02969>
- [25] Cao, Jie, Jia Wang, Xiujun Wang, Jian Zhang, Kun Liu, Yixin Wang, Weikun Zhen, and Yingpeng Chen. "Preparation and characterization of modified amphiphilic nano-silica for enhanced oil recovery." *Colloids and Surfaces A: Physicochemical and Engineering Aspects* 633 (2022): 127864. <https://doi.org/10.1016/j.colsurfa.2021.127864>
- [26] Chandio, Tariq Ali, Muhammad A. Manan, Khalil Rehman Memon, Ghulam Abbas, and Ghazanfer Raza Abbasi. "Enhanced oil recovery by hydrophilic silica nanofluid: experimental evaluation of the impact of parameters and mechanisms on recovery potential." *Energies* 14, no. 18 (2021): 5767. <https://doi.org/10.3390/en14185767>
- [27] Li, Shidong, Luky Hendraningrat, and Ole Torsaeter. "Improved oil recovery by hydrophilic silica nanoparticles suspension: 2 phase flow experimental studies." In *IPTC 2013: International Petroleum Technology Conference*, pp. cp-350. European Association of Geoscientists & Engineers, 2013. <https://doi.org/10.2523/16707-MS>